Key Engineering Materials Vols. 651-653 (2015) pp 1197-1203
© (2015) Trans Tech Publications, Switzerland
doi:10.4028/www.scientific.net/KEM.651-653.1197

Submitted: 2014-12-01
Revised: 2015-02-14
Accepted: 2015-02-15

Comparison of several behaviour laws intended to produce a realistic Ti6Al4V chip by finite elements modelling

François Ducobu[1,a], Pedro-José Arrazola[2,b], Edouard Rivière-Lorphèvre[1,c], and Enrico Filippi[1,d]

[1]University of Mons, Faculty of Engineering, Machine Design and Production Engineering Department - Belgium

[2]Mondragon University, Faculty of Engineering, Mechanical and Manufacturing Department - Spain

[a]Francois.Ducobu@umons.ac.be, [b]pjarrazola@mondragon.edu, [c]Edouard.Riviere@umons.ac.be, [d]Enrico.Filippi@umons.ac.be

Keywords: Behaviour law, finite elements modelling, saw-toothed chip, Ti6Al4V.

Abstract. The final aim of finite elements modelling is to help in the choice of the cutting parameters and in the comprehension of the involved phenomena. Representing correctly the behaviour of the machined material is hard due to the extreme conditions encountered, although this is a key parameter to develop a realistic model. Four laws are used in this paper to represent the Ti6Al4V. They are all based on the Johnson-Cook law. This study shows that the influence of the behaviour law is high on the chip morphology and on the forces and that the strain softening phenomenon should be taken into account. For the cutting conditions adopted, it is however necessary to add damage properties in the chip to obtain a morphology and a cutting force evolution close to the experimental reference.

Introduction

Machining is a complex operation that can be assisted by finite elements modelling to enhance the comprehension of the phenomena it involves. It is also intended to help the practitioner in the choice of the adequate cutting parameters. The development of realistic finite elements models requires to model correctly the machined material in very severe conditions of strain, strain rate and temperature. These extreme conditions can, however, not be reached by current experimental means of tests. The deduced constitutive laws do therefore only represent partially the material behaviour. It is particularly observed for the Johnson-Cook law, although it is the most used in the field and consequently also for Ti6Al4V, the machined material considered in this work. In order to solve this issue, several laws have been introduced recently. They, amongst others, take into account the strain softening, contributing to the formation of saw-toothed Ti6Al4V chip. The parameters of these laws are usually obtained through inverse analysis thanks to the observation of the experimental chips. It implies that the user misses objective arguments to choose between these laws in the absence of experimental reference curves. This article proposes to compare these behaviour laws by introducing them in a finite elements model. The results are then opposed to an experimental case obtained by strictly orthogonal cutting conditions in order to highlight the differences they lead to and help to choose which one should be adopted for future modelling.

Experimental setup

The machined material is the titanium alloy Ti6Al4V. It is mainly used in the annealed state. Ti6Al4V grade 5 (ASM 4928) at the classic state used in the aerospace industry (annealed at 750°C for one hour followed by air cooling) was considered in this study. In order to have an experimental reference in orthogonal cutting and in the same cutting conditions, the experimental orthogonal cutting setup introduced in [1] was adopted. It used a standard milling machine as a planning machine. The sample to machine is inserted into the spindle and the tool is fixed with a custom made support piece on the

force sensor on the machine table. The cutting movement is the sample horizontal displacement with respect to the stationary tool. This allows to remove a layer of material of variable thickness in strictly orthogonal cutting conditions. In this configuration, the maximal achievable cutting speed is set by the maximal feed rate of the milling machine; typically of the order of 20 m/min to 30 m/min. The cutting length and the width of cut are set by the dimensions of the feature to machine. In this case, it consists of a 10 mm long and 1 mm wide tenon. This cutting length is large enough for the process to be steady and the forces to be measured, while it is short enough to prevent the chip to roll up. It can therefore be embedded without unrolling, and there is no error on the measured lengths due to the unrolling distortions. A width of 1 mm minimizes the efforts in the spindle bearings and it directly gives the forces value per mm width as in 2D plane strain numerical models (with a width of cut to depth of cut ratio larger than 3). The cutting conditions were chosen to provide the same characteristics as the numerical model used by Ducobu et al. [2]. The rake angle is 15°, the clearance angle 2° and the cutting edge radius 20 µm. The cutting speed is fixed at 30 m/min and the depth of cut is 0.28 mm.

Numerical model

Model presentation. The numerical model consists of a 2D plane strain explicit Lagrangian orthogonal cutting model developed with the commercial software ABAQUS/Explicit v6.11. It classically takes into account the area close to the cutting edge of the tool. The workpiece is modelled as a rectangular block of 1 mm long and 0.75 mm high, while the tool is modelled with the same geometry as for the experiments. These two parts are meshed with four-node CPE4RT linear elements. The workpiece is fixed in space while the tool moves horizontally at the cutting speed (30 m/min). The workpiece material is Ti6Al4V, assumed to be homogeneous. Its behaviour is described by four different laws, as detailed in the next paragraph. The tool material, tungsten carbide, is also homogeneous and its behaviour is described by a linear elastic law. Coulomb's friction is used to model friction at the tool – chip interface, all the friction energy is converted into heat (classical assumption) and this heat flows equally to the workpiece and the tool. The workpiece and tool initial temperature is set to 25°C. Only conduction is considered and all the parts faces are adiabatic. Due to the Lagrangian formulation, an "eroding element" chip separation criterion is introduced. This separation criterion is based on crack propagation depending on the stress and strain state of the machined material. This chip formation approach, by ductile failure phenomenon, is composed of two steps. In the first one, a damage initiation criterion must be fulfilled. The damage initiation criterion adopted is the Johnson-Cook shear failure model [3]. The second step concerns damage evolution, based on the fracture energy approach. This criterion uses the fracture energy, G_f, which is the required energy to open a unitary area crack. After damage initiation, the material behaviour is represented by a stress-displacement relation rather than a stress-strain relation [4]. As soon as the specified value of G_f is reached in a finite element, it is deleted and all of its stress components are put to zero. The suppression of a finite element introduces a crack in the workpiece, making it possible for the chip to come off. In this model, the chip separation is assumed to occur along a straight path composed of one element in height. Damage properties are therefore given only to this part of the workpiece, typically called "sacrificial layer" [5].

Behaviour laws. Four laws are considered in this work to represent the behaviour of the Ti6Al4V. The first one is the Johnson-Cook (JC) law, the most adopted law in machining modelling. Its flow stress is described by [6]:

$$\sigma = (A + B\,\varepsilon^n)\left(1 + C\,\ln\frac{\dot{\varepsilon}}{\dot{\varepsilon}_0}\right)\left(1 - \left[\frac{T - T_{room}}{T_{melt} - T_{room}}\right]^m\right). \quad (1)$$

The parameters chosen for this study come from Meyer et al. [7], as in [2].
The second one is the Hyperbolic TANgent (TANH) law, which is a JC law modified by Calamaz et al. [8] to take into account the strain softening phenomenon that would be necessary to produce saw-toothed Ti6Al4V chips. It has the following expression [8]:

$$\begin{aligned}\sigma &= \left[A + B\,\varepsilon^n \left(\frac{1}{\exp\left(\varepsilon^a\right)}\right)\right]\left[1 + C\,\ln\frac{\dot{\varepsilon}}{\dot{\varepsilon}_0}\right] \\ &\quad \left[1 - \left(\frac{T - T_{room}}{T_{melt} - T_{room}}\right)^m\right]\left[D + (1-D)\tanh\left(\frac{1}{(\varepsilon + S)^c}\right)\right]\end{aligned} \tag{2}$$

with

$$D = 1 - \left(\frac{T}{T_{melt}}\right)^d \quad \text{and} \quad S = \left(\frac{T}{T_{melt}}\right)^b.$$

The set of parameters of the TANH law comes from Calamaz et al. [8].
The third one is a second version of the TANH law, called TANHb in this article. According to Calamaz et al. [9], it improves the first TANH formulation in the sense that the strain softening appears from approximately T_{rec} (0.3 times the melting temperature) and not at room temperature any more. This law is given by [9]:

$$\sigma = \left[A + B\,\varepsilon^n\right]\left[1 + C\,\ln\frac{\dot{\varepsilon}}{\dot{\varepsilon}_0}\right]\left[1 - \left(\frac{T - T_{room}}{T_{melt} - T_{room}}\right)^m\right]\left[E + (1-E)\tanh\left(\frac{1}{\varepsilon + \varepsilon_0}\right)\right] \tag{3}$$

with

$$E = 1 - \left(\frac{p\,\varepsilon}{1 + p\,\varepsilon}\tanh\left(\frac{T - T_{room}}{T_{rec} - T_{room}}\right)^q\right).$$

The parameters adopted come from [9]. The additional parameters, by comparison with the JC law, of both TANH laws were obtained by Calamaz et al. through inverse analysis based on experimental cutting results.
The fourth one is another modification of TANH law by Sima and Özel [10] (called Sima's law in this article). This consists of a TANH law with a control on the *tanh* function, and therefore the thermal softening [10]:

$$\begin{aligned}\sigma &= \left[A + B\,\varepsilon^n \left(\frac{1}{\exp\left(\varepsilon^a\right)}\right)\right]\left[1 + C\,\ln\frac{\dot{\varepsilon}}{\dot{\varepsilon}_0}\right] \\ &\quad \left[1 - \left(\frac{T - T_{room}}{T_{melt} - T_{room}}\right)^m\right]\left[D + (1-D)\left\{\tanh\left(\frac{1}{(\varepsilon + S)^c}\right)\right\}^p\right].\end{aligned} \tag{4}$$

The parameters of this law are given by Sima and Özel [10].
The four laws are plotted in Fig. 1 at a strain rate of 10,000 s^{-1} and a temperature of 573 K (below T_{rec} = 600 K); the temperature is set to 773 K (above T_{rec}) in Fig. 2.

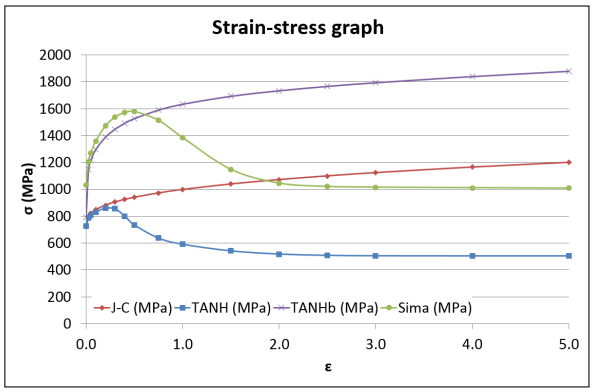

Fig. 1: Flow stress curves at 573 K and 10,000 s^{-1}

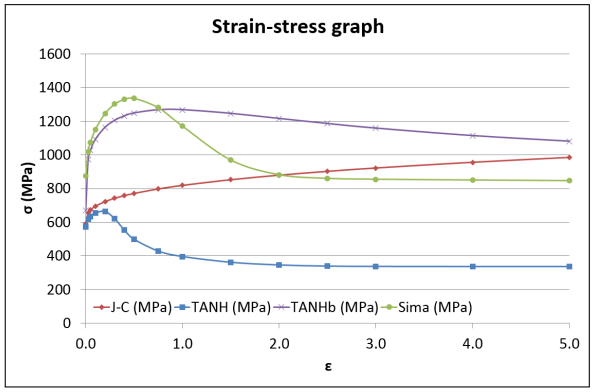

Fig. 2: Flow stress curves at 773 K and 10,000 s^{-1}

As the temperature is higher in Fig. 2, lower stresses were expected and the strain softening is also observed for TANHb law. Its shape is different of TANH and Sima's laws. The evolutions of TANH and Sima's laws are quite close to each other, the main difference being the level of the stresses (which is also observed for TANHb law) and the strain softening occurring at lower strain for TANH law. The comparison between JC and TANH laws at 573 K clearly shows the influence of the strain softening on the level of the stresses. Different stresses level will end in different cutting forces levels.

Results

Without damage in the chip. The experimental chips were saw-toothed as expected. They were etched and polished before observation with an optical microscope. To characterize the chip geometry, four lengths (highlighted in Fig. 3 (a)) are usually measured [11]: the undeformed chip length L, the height of the teeth H, the valley C and the pitch P. When looking at the chips morphologies from the

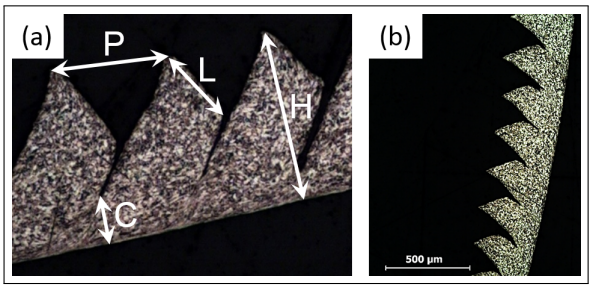

Fig. 3: (a) Characteristic lengths of a saw-toothed chip (b) Experimental chip

modelling in Fig. 4, it is clear that they are all far away from the experimental one and it does not make sense to measure their characteristic lengths. Some differences between the chips are however observed. The chips from JC and TANHb laws are continuous, while they have small teeth with TANH and Sima's law. The two first teeth with TANH law and the first one with Sima's law are different of the next ones, this is due to the unsteady chip formation at the beginning of the cut.

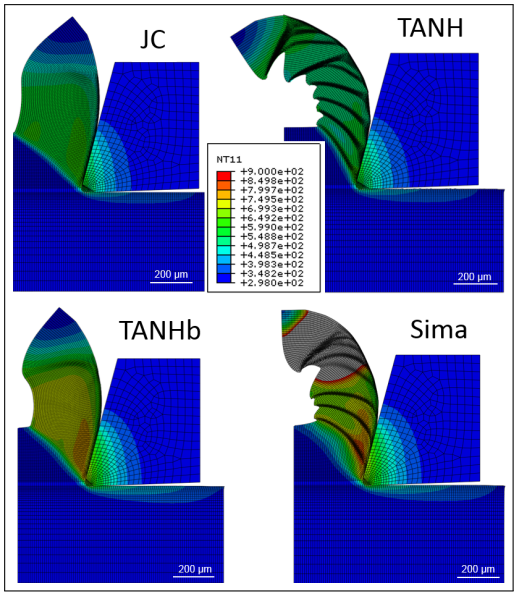

Fig. 4: Numerical chips without damage, temperature plots (in K)

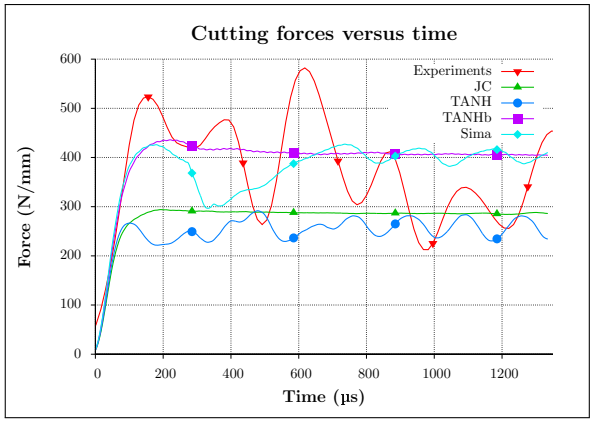

Fig. 5: Cutting forces without damage in the chip

These differences are also noted on the forces evolutions plotted in Fig. 5 for each numerical case and the experimental one. The forces evolutions are closely linked to the chip morphology. Indeed, the cutting force is constant when the chip is continuous and has a cyclic evolution in regime when it is saw-toothed. The level of the forces is different. It is closely linked to the behaviour law: when the level of the stresses is higher, the magnitude of the cutting force is higher as well. Looking at Fig. 1, it becomes evident that the absence of teeth in the chip is due to the strain softening not taken into account in the behaviour law or to the temperature too low to activate it (Fig. 2). All these cutting forces evolutions are very different of that measured experimentally. The RMS values of the forces are compared in Table 1. As it could be assumed from Fig. 5, TANHb and Sima's laws lead to RMS values closer to that of the experiments. The numerical chips obtained up to now have a morphology

Table 1: Characteristic lengths with damage in the chip and RMS cutting forces values, closest values to experimental ones in bold

	L [µm]	H [µm]	C [µm]	P [µm]	CF [N/mm]	CF with dam. [N/mm]
Experiment	206 ± 17	288 ± 14	157 ± 21	233 ± 17	387	387
JC	-	-	-	-	288	256
TANH	104	245	**164**	105	260	224
TANHb	**173**	**296**	76	**138**	412	**306**
Sima	136	279	66	91	**405**	273

far from the experimental one. For the cutting conditions adopted, the behaviour laws considered do therefore not allow to produce a satisfactory chip. In accordance with the experimental observations [1], damage will be introduced in the chip to obtain a morphology closer to the experiments [2, 8].

With damage in the chip. When introducing damage in the chip, it is expected to obtain chips with a smaller valley, particularly with the TANH law and Sima's law, as small teeth were observed previously. Fig. 6 shows the corresponding four numerical chips. The three ones with a behaviour law taking strain softening into account exhibit a saw-toothed morphology. With TANHb law and Sima's law, the chips are qualitatively very close. Such a chip with TANHb law was not expected when look-

ing at the results without damage. That morphology change is mostly due to the larger deformation in the primary shear band involved by the crack propagation and inducing an increase of the temperature, turning on the strain softening.

The characteristic lengths are given in Table 1 (the first tooth of each chip is not taken into account).

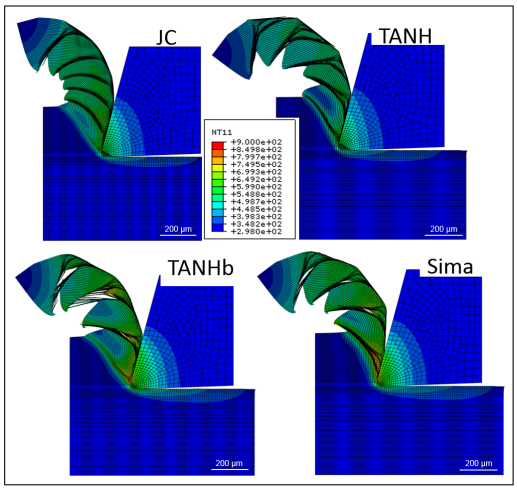

Fig. 6: Chips with damage, temperature plots (in K)

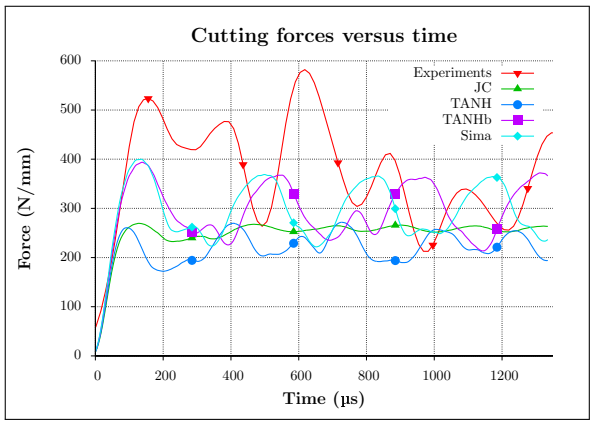

Fig. 7: Cutting forces with damage in the chip

The chip with the closest lengths to the experimental one is that with TANHb law. The undeformed tooth length is slightly underestimated, while the height of the teeth is close to the experiments. The valley is half that of the reference one, indicating that the crack propagates too easily in the primary shear zone. Such a small valley leads to a chip with a low rigidity, which is probably the main reason for the low value of the pitch. In Fig. 7, it is seen that none of the cutting forces evolutions is constant any more. They can be linked to the teeth formation: a decrease in the force corresponds to the formation of a tooth. The teeth are much larger which leads to a higher magnitude of the forces variations. As without damage in the chip, TANH and Sima's laws lead to a higher cutting force. The comparison of the experimental force evolution with that of TANHb and Sima's shows that their mean level seems lower, as well as the amplitude of the variations. The RMS values (Table 1) confirm that the numerical levels are lower than the measured one. The behaviour law leading to the closest cutting force is the TANHb law.

Conclusions

The behaviour law has a strong influence on the chip formation and the level of the cutting force. The absence of damage properties in the chip shows the specificities of each law but they are not sufficient, in these cutting conditions, to form a saw-toothed chip close to the experimental reference. This study shows that the strain softening is not a negligible factor in the formation of a saw-toothed chip. It also confirms that the crack propagation in the chip is a necessary feature to form a chip with a morphology close to the experimental one. Although some differences are still noticed for the morphology, as well as for the cutting force, in the cutting conditions adopted in this paper, the TANHb behaviour law lead to the closest results to the experiments.

Acknowledgements

The authors thank the *Fonds de la Recherche Scientifique de Belgique* (FRS-FNRS), Wallonie- Bruxelles International (*Bourse d'excellence WBI.World*) and the projects InProRet (code IE12-342), InProRet II (code IE13-365) for the financial support provided for the research presented trough this paper.

References

[1] F. Ducobu, E. Rivière-Lorphèvre and E. Filippi: Int. J. Mater. Form. (2014).

[2] F. Ducobu, E. Rivière-Lorphèvre and E. Filippi: Int. J. Mech. Sc. 81 (2014) 77-87.

[3] G. Johnson and W. Cook: EFM. 21 (1985) 31-48.

[4] T. Mabrouki, F. Girardin, M. Asad and J.-F. Rigal: Int. J. Mach. Tools and Manuf. 48 (2008) 1187-1197.

[5] S. Subbiah and S. Melkote: Mater. Sc. Eng. A. 474 (2008), 283-300.

[6] G. Johnson: NSWC TR 86-144 (1985).

[7] H. W. Meyer and D. S. Kleponis: Int. J. Impact Eng. 26 (2001) 509-521.

[8] M. Calamaz, D. Coupard and F. Girot: Int. J. Mach. Tools and Manuf. 48 (2008) 275-288.

[9] M. Calamaz, D. Coupard and F. Girot: Mach. Sc. and Technol. 14 (2010) 244-257.

[10] M. Sima and T. Özel: Int. J. Mach. Tools and Manuf. 50 (2010) 943-960.

[11] D. Umbrello: J. of Mater. Proc. Technol. 196 (2008) 79-87.